TPL2 mediates autoimmune inflammation through activation of the TAK1 axis of IL-17 signaling

Yichuan Xiao,[1] Jin Jin,[1] Mikyoung Chang,[1] Mako Nakaya,[1] Hongbo Hu,[1] Qiang Zou,[1] Xiaofei Zhou,[1] George C. Brittain,[1] Xuhong Cheng,[1] and Shao-Cong Sun[1,2]

[1]Department of Immunology, the University of Texas MD Anderson Cancer Center, Houston, TX 77030
[2]The University of Texas Graduate School of Biomedical Sciences at Houston, Houston, TX 77030

Development of autoimmune diseases, such as multiple sclerosis and experimental autoimmune encephalomyelitis (EAE), involves the inflammatory action of Th1 and Th17 cells, but the underlying signaling mechanism is incompletely understood. We show that the kinase TPL2 is a crucial mediator of EAE and is required for the pathological action of Th17 cells. TPL2 serves as a master kinase mediating the activation of multiple downstream pathways stimulated by the Th17 signature cytokine IL-17. TPL2 acts by linking the IL-17 receptor signal to the activation of TAK1, which involves a dynamic mechanism of TPL2–TAK1 interaction and TPL2-mediated phosphorylation and catalytic activation of TAK1. These results suggest that TPL2 mediates TAK1 axis of IL-17 signaling, thereby promoting autoimmune neuroinflammation.

CORRESPONDENCE
Shao-Cong Sun:
ssun@mdanderson.org

Abbreviations used: CNS, central nervous system; EAE, experimental autoimmune encephalomyelitis; IB, immunoblot; IKK, IκB kinase; IP, immunoprecipitation; MOG, myelin oligodendrocyte glycoprotein; MS, multiple sclerosis; QPCR, quantitative RT-PCR.

IL-17, also called IL-17A, is a signature cytokine produced by Th17 cells, a lineage of $CD4^+$ effector T cells which mediates both host defense against infections and autoimmune inflammatory diseases, such as multiple sclerosis (MS) and rheumatoid arthritis (Iwakura et al., 2011). MS is a chronic disease of the central nervous system (CNS), characterized by inflammation, demyelination, and axonal damage (Compston and Coles, 2008). Although the etiology of MS remains unclear, it is widely considered to be an autoimmune disorder influenced by both environmental and genetic factors (Simmons et al., 2013). Studies using an animal model of MS, the experimental autoimmune encephalomyelitis (EAE), suggest the crucial involvement of myelin-specific T cells, particularly the IL-17–producing Th17 cells (Simmons et al., 2013). Upon activation in the peripheral lymphoid organs, these autoimmune T cells enter the CNS and become reactivated by resident antigen-presenting cells, leading to the production of IL-17 and related cytokines. These T cell–derived cytokines contribute to the activation of CNS-resident cells and to the induction of leukocyte infiltration into the CNS, culminating in disseminated CNS inflammation, demyelination, and the development of disease symptoms (Goverman, 2009).

IL-17 is the prototypical member of a family of related cytokines and has been linked to the pathogenesis of both MS and other autoimmune diseases (Gaffen, 2009; Iwakura et al., 2011; Zepp et al., 2011; Song and Qian, 2013). The expression level of IL-17 is elevated in MS patients, and genome-wide association studies suggest the linkage of the IL-17 and IL-17R genes with MS (Matusevicius et al., 1999; Sawcer et al., 2011; Muls et al., 2012). In addition to the Th17 cells, several other cell types, such as lymphoid tissue inducer–like cells, γδ T cells, $CD8^+$ T cells, and nature killer T cells, produce IL-17 (Iwakura et al., 2011). IL-17 stimulates the expression of chemokines and proinflammatory cytokines in several cell types, including fibroblasts, endothelial cells, epithelial cells, and astrocytes (Zepp et al., 2011). Genetic evidence suggests that IL-17 signaling in neuroectoderm-derived CNS-resident cells, particularly astrocytes, plays a crucial role in mediating EAE pathogenesis (Kang et al., 2010). IL-17–stimulated production of chemokines and proinflammatory cytokines in the

The Rockefeller University Press $30.00
J. Exp. Med. 2014 Vol. 211 No. 8 1689-1702
www.jem.org/cgi/doi/10.1084/jem.20132640

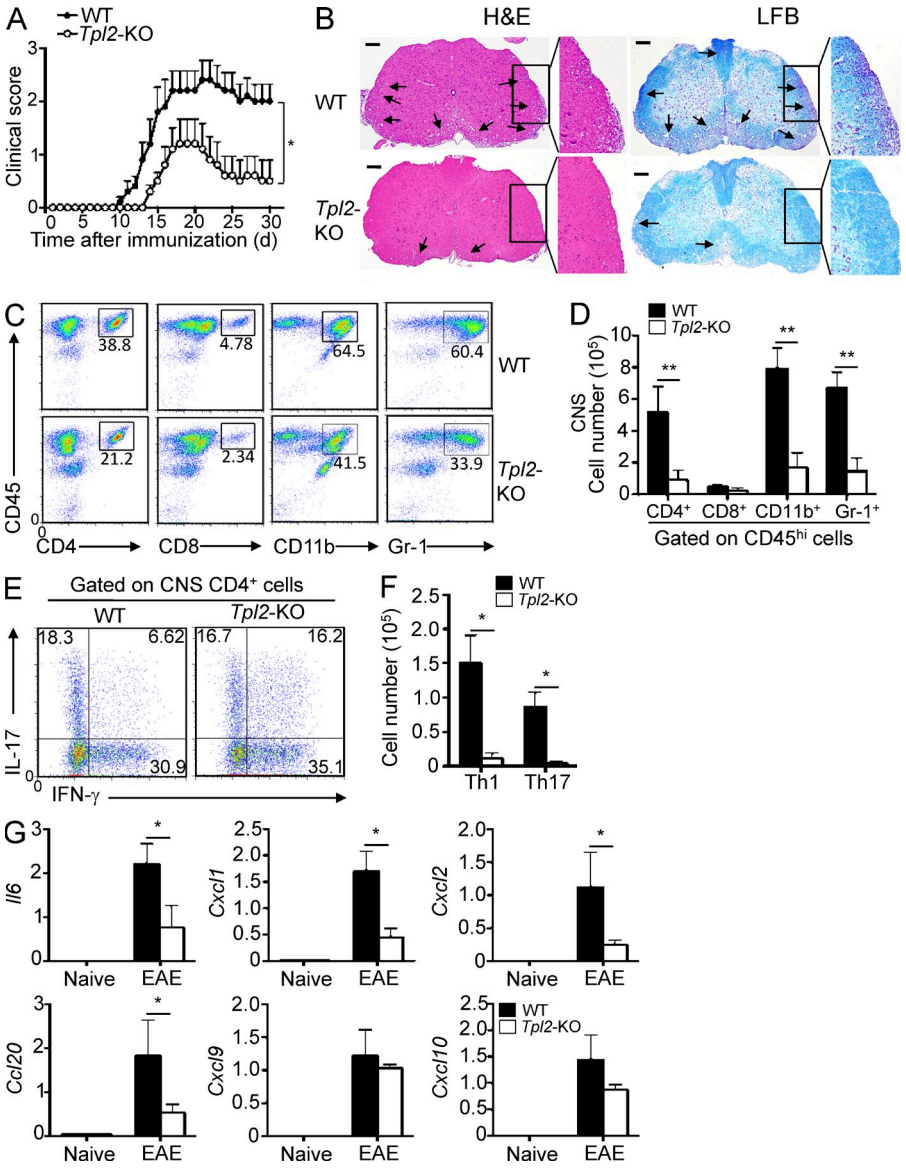

Figure 1. *Tpl2*-KO mice are resistant to CNS inflammation. (A) Mean clinical scores of age- and sex-matched WT and *Tpl2*-KO mice subjected to MOG_{35-55}-induced EAE ($n = 6$ mice per group). (B) H&E and Luxol Fast Blue (LFB) staining of spinal cord sections from MOG_{35-55}-immunized WT and *Tpl2*-KO EAE mice for visualizing immune cell infiltration and demyelination, respectively (arrows). Bars, 100 µm. (C and D) Flow cytometric analyses of $CD4^+$ and $CD8^+$ T cells, $CD11b^+$ monocytes, and $Gr\text{-}1^+$ neutrophils among the $CD45^+$ immune cells infiltrating to the CNS (brain and spinal cord) of MOG_{35-55}-immunized WT and *Tpl2*-KO mice ($n = 5$ mice per group, day 15 after immunization). Data are presented as a representative plot (C) and summary graph of the absolute cell numbers (D). (E and F) Infiltrating immune cells isolated from CNS (brain and spinal cord) of MOG_{35-55}-immunized WT and *Tpl2*-KO mice ($n = 5$ mice per group, day 15 after immunization) were fixed and permeabilized, and $CD4^+$ T cells were analyzed by flow cytometry for intracellular IFN-γ and IL-17. Data are presented as a representative plot (E) and summary graph of the absolute cell numbers (F). (G) QPCR analysis to determine the relative mRNA expression level of proinflammatory genes in spinal cords of unimmunized (naive) and MOG_{35-55}-immunized (EAE) WT and *Tpl2*-KO mice ($n = 4$ mice per group, day 15 after immunization). Data were normalized to a reference gene, *Actb*. *, $P < 0.05$; **, $P < 0.01$. Data are representative of three or more independent experiments. Error bars are mean ± SD values.

CNS-resident cells mediates leukocyte recruitment during the induction of CNS inflammation.

Signal transduction from the IL-17R involves recruitment of the E3 ubiquitin ligase TRAF6 (Schwandner et al., 2000). The cytoplasmic region of IL-17R contains a signaling domain, the SEF/IL-17R domain, which interacts with the adaptor protein ACT1 (also called CIKS) in response to IL-17 stimulation (Novatchkova et al., 2003; Chang et al., 2006; Qian et al., 2007). In turn, ACT1 recruits TRAF6 to the IL-17R and triggers the activation of several downstream signaling factors, including IκB kinase (IKK) and its target transcription factor NF-κB, the MAP kinases JNK and p38, and the transcription factor C/EBP (Qian et al., 2007; Liu et al., 2009). Conversely, ACT1 and TRAF6 are largely dispensable for IL-17–stimulated activation of the MAP kinase ERK (Qian et al., 2007; Liu et al., 2009). In addition to the activation of TRAF6, ACT1 also recruits TRAF2 and TRAF5 via a mechanism that depends on IKKi-mediated ACT1 phosphorylation (Bulek et al., 2011; Song and Qian, 2013). The TRAF2/5 pathway plays an important role in IL-17–stimulated stabilization of mRNAs for specific target genes (Bulek et al., 2011; Sun et al., 2011).

The mechanism by which IL-17R signal is transduced to the various downstream pathways, particularly the MAPK pathways, has not been fully elucidated (Song and Qian, 2013). What is currently known is that the protein kinase TAK1 is recruited to the IL-17R signaling complex and is required for IL-17–stimulated gene expression (Qian et al., 2007). A recent gene-silencing study suggested that TAK1 is important for IL-17–stimulated activation of NF-κB (Zhu et al., 2012), but how TAK1 is activated by the IL-17R signaling and whether TAK1 also plays a role in regulating other signaling pathways remain unclear.

In the present study, we obtained genetic evidence that TAK1 mediates IL-17–stimulated activation of both NF-κB

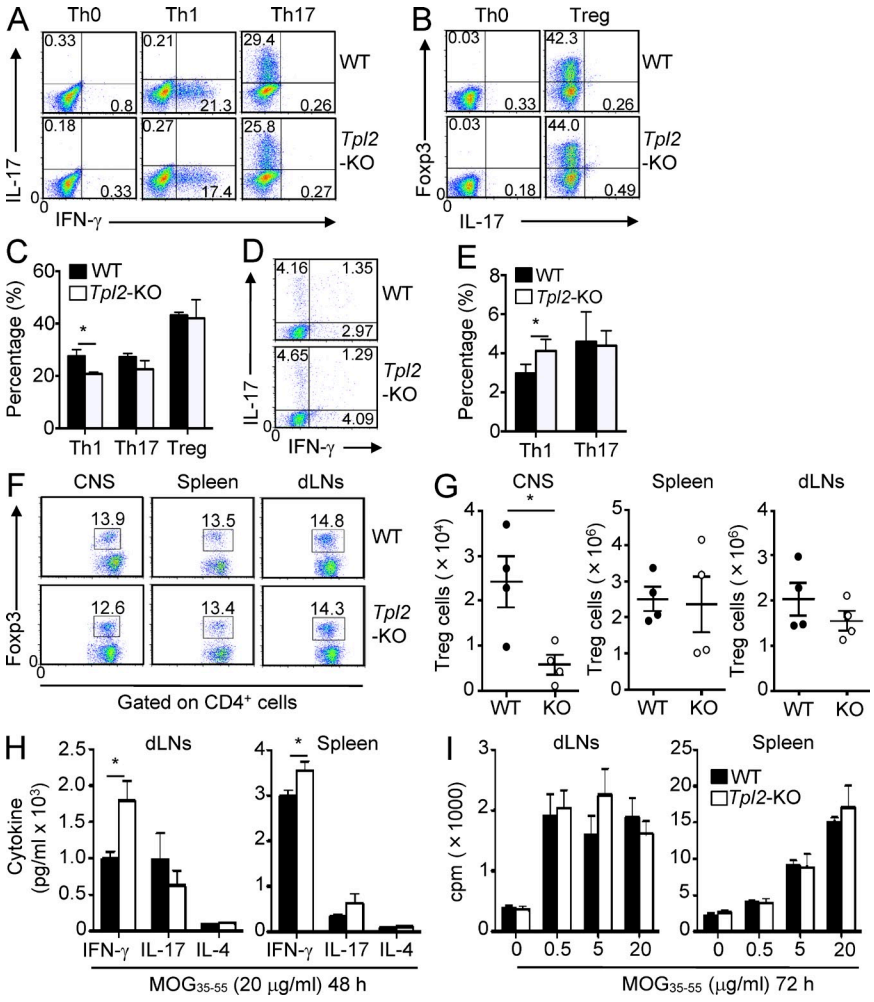

Figure 2. TPL2 deficiency does not compromise T cell differentiation or recall responses. (A–C) Naive splenic CD4+ T cells ($CD44^{lo}CD62L^{hi}$) isolated from WT and *Tpl2*-KO mice were stimulated for 4 d with 5 µg/ml of plate-bound anti-CD3 and 1 µg/ml anti-CD28 under Th0, Th1, Th17, or T reg conditions as described in Materials and methods. Flow cytometry was used to measure the frequency of IFN-γ– and IL-17–producing cells, and Foxp3+ cells, showing a representative plot (A and B) and a summary graph (C). (D and E) Flow cytometry analysis of IFN-γ– and IL-17–producing cells in the draining LNs of day 15 MOG_{35-55}-immunized WT and *Tpl2*-KO mice, showing a representative plot (D) and a summary graph (E). Data are representative of 4 animals. (F and G) Flow cytometry analysis of CD4+Foxp3+ T reg cells in the CNS, spleen, and draining LNs of day 15 MOG_{35-55}-immunized WT and *Tpl2*-KO mice, showing a representative plot of T reg cell frequency (F) and a summary graph of T reg cell number (G). Data are representative of 4 animals per group. (H and I) Draining LN cells or splenocytes isolated from day 15 MOG_{35-55}-immunized WT or *Tpl2*-KO mice were restimulated in vitro with the MOG peptide at the indicated concentrations and time periods. Supernatants were subjected to ELISA of the indicated cytokines (H), and cell proliferation was measured based on ^{3}H-thymidine incorporation. *, $P < 0.05$. Data are representative of two (A–C, F, and G) or at least three (D, E, H, and I) independent experiments. Error bars are mean ± SD values.

and two major MAPKs: JNK and p38. More importantly, we identified the serine/threonine kinase TPL2 as a pivotal mediator of TAK1 activation in the IL-17R signaling pathway. TPL2 is known as a kinase that selectively mediates ERK activation by TLRs and has been implicated in inflammation (Gantke et al., 2011; Vougioukalaki et al., 2011). Unexpectedly, in the IL-17R pathway, we found that TPL2 was completely dispensable for ERK activation but was required for the activation of NF-κB, JNK, and p38. In response to IL-17 stimulation, TPL2 bound to TAK1 and mediated the phosphorylation and catalytic activity of TAK1. The TPL2 deficiency severely inhibited the IL-17–stimulated expression of chemokines and proinflammatory cytokines in astrocytes, and the *Tpl2*-KO mice were refractory to EAE induction due to attenuated leukocyte recruitment to the CNS. Given the involvement of IL-17 signaling in various inflammatory diseases, these findings not only provide novel insight into the mechanism of IL-17R signaling but also have profound implications for therapeutic approaches.

RESULTS

TPL2 is a crucial mediator of EAE pathogenesis

To investigate the role of TPL2 in regulating autoimmune inflammation, we examined the effect of TPL2 deficiency on the pathogenesis of EAE. Immunization of WT mice with a myelin oligodendrocyte glycoprotein (MOG) peptide ($MOG_{35–55}$), along with an injection of pertussis toxin, led to the induction of severe EAE clinical scores (Fig. 1 A). Compared with the WT mice, the *Tpl2*-KO mice were more resistant to EAE induction, as revealed by reduced clinical scores (Fig. 1 A) and diminished inflammation and demyelination (Fig. 1 B). Consistently, during the effector phase of EAE induction, *Tpl2*-KO mice had a marked reduction in the percentage (Fig. 1 C) and number (Fig. 1 D) of CNS-infiltrating immune cells, including $CD4^+$ and $CD8^+$ T cells, $CD11b^+$ monocytes, and $Gr1^+$ neutrophils. Within the CNS-infiltrating $CD4^+$ T cell population, the percentages of $IL\text{-}17^+$ Th17 cells and $IFN\text{-}\gamma^+$ Th1 cells in the *Tpl2*-KO were similar to or even higher than that of the WT mice (Fig. 1 E). However, due to the overall attenuation of immune cell recruitment to the CNS, the absolute numbers of both Th1 and Th17 cells were greatly reduced in the CNS of *Tpl2*-KO mice (Fig. 1 F). We found that the CNS tissue of the $MOG_{35–55}$-immunized *Tpl2*-KO mice had reduced expression of the proinflammatory cytokine IL-6 and several chemokines known to mediate immune cell recruitment (Fig. 1 G). These results suggest a role for TPL2 in mediating the activation or CNS recruitment of inflammatory immune cells.

TPL2 is dispensable for effector T cell differentiation and activation

EAE induction involves the generation of CNS-specific autoimmune effector T cells, including IL-17–producing Th17 cells and IFN-γ-producing Th1 cells (Simmons et al., 2013). Thus, the EAE-refractory phenotype of the *Tpl2*-KO mice could be due to a defect in the activation of $MOG_{35–55}$-specific effector T cells or attenuated responses of CNS cells involved in CNS inflammation and leukocyte recruitment. To test the former possibility, we performed an in vitro naive $CD4^+$ T cell activation assay. We found that the Tpl2 ablation had little or no effect on the production of Th17 effector cells or the regulatory T (T reg) cells (Fig. 2, A–C). In agreement with a previous study (Watford et al., 2008), the *Tpl2*-KO CD4 naive T cells had a defect in the production of Th1 cells (Fig. 2, A and C). However, the *Tpl2*-KO mice did not show any obvious defect in the in vivo production of Th1 or Th17 cells during the effector phase of EAE induction (Fig. 2, D and E). In fact, we detected a moderately higher frequency of Th1 cells in the draining lymph nodes of the EAE-induced Tpl2-KO mice (Fig. 2, C and D), although the underlying mechanism remains to be examined. The frequency of T reg cells was comparable between the WT and *Tpl2*-KO mice (Fig. 2 F). Although the absolute number of T reg cells was reduced in the CNS (Fig. 2 G), this was apparently due to the reduction in the total T cell number (Fig. 1 D). The T cells isolated from the draining lymph nodes and spleen of the *Tpl2*-KO mice were also competent in antigen-stimulated recall responses, as revealed by cytokine production (Fig. 2 H) and proliferation (Fig. 2 I) assays. Consistent with the flow cytometry assays (Fig. 2 E), the *Tpl2*-KO T cells produced a higher level of secreted IFN-γ (Fig. 2 H). Overall, these results suggest that TPL2 is dispensable for activation and differentiation of $MOG_{35–55}$-specific inflammatory T cells.

TPL2 functions in nonhematopoietic cells to mediate leukocyte recruitment and EAE pathogenesis

To examine whether TPL2 functions in hematopoietic cells or the radioresistant nonhematopoietic cells, we generated bone marrow–chimeric mice by adoptively transferring WT or *Tpl2*-KO bone marrow cells into lethal dose–irradiated WT recipient mice. When reconstituted with either the WT bone marrow or the *Tpl2*-KO bone marrow, the recipient mice were competent in EAE induction (Fig. 3 A). The recipients of the WT and *Tpl2*-KO bone marrows also had comparable levels of immune cell infiltration into the CNS (Fig. 3, B and C). Furthermore, the WT and *Tpl2*-KO $CD4^+$ T cells also displayed comparable ability to mediate EAE induction when they were adoptively transferred into *Rag1*-KO mice (Fig. 3 D). As a complementary approach, we adoptively transferred WT bone marrow into lethal dose–irradiated WT or *Tpl2*-KO mice. Even after being reconstituted with the WT bone marrow, the *Tpl2*-KO mice were still more refractory to EAE induction than WT mice (Fig. 4 A). These data suggest that TPL2 functions in the radioresistant nonhematopoietic cells to regulate EAE pathogenesis.

To analyze immune cell recruitment into the CNS, we used WT bone marrow from GFP transgenic mice as donor cells in the adoptive transfer experiments. Thus, the bone marrow chimeric mice would have their peripheral immune cells replaced with GFP^+ immune cells. Before immunization, the WT and *Tpl2*-KO chimeric mice contained comparable frequency of GFP^+ immune cells in the spleen (Fig. 4 B). However, during the effector phase of EAE induction (day 15 after immunization), the WT recipient mice had massive CNS infiltration with the GFP^+ immune cells (Fig. 4 C), whereas the *Tpl2*-KO chimeric mice showed a drastic reduction in both the frequency (Fig. 4 C) and the absolute number (Fig. 4 D) of the CNS-infiltrating immune cells. By gating to the GFP^+ cells, we found that the CNS infiltration of both $CD4^+$ and $CD8^+$ T cells was severely attenuated in the *Tpl2*-KO chimeric mice (Fig. 4, E and F). Although the frequency of Th1 and Th17 cells within the CNS $CD4^+$ T cell population was similar between the WT and *Tpl2*-KO chimeric mice (Fig. 4 G), the absolute number of both Th1 and Th17 cells was substantially reduced in the *Tpl2*-KO CNS (Fig. 4 H).

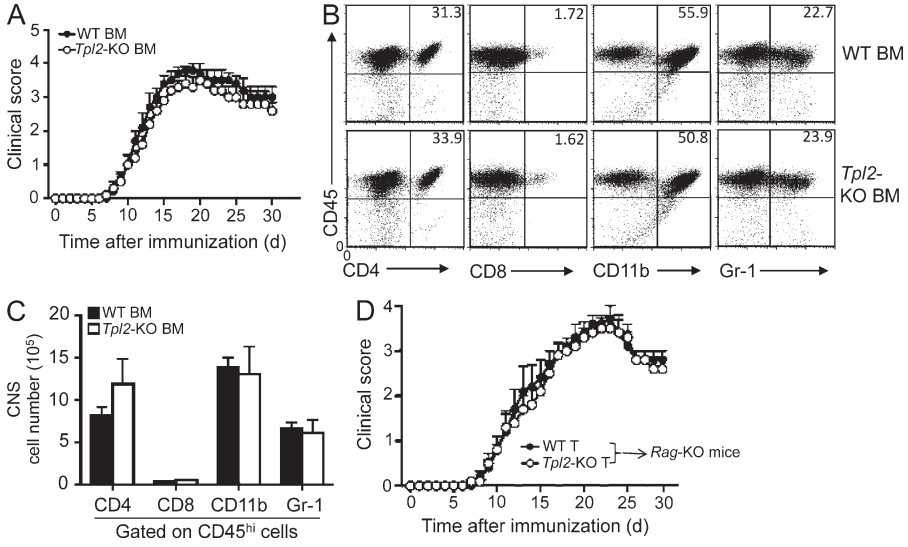

Figure 3. Tpl2 is dispensable in hematopoietic cells for EAE pathogenesis. (A) Mean clinical score after EAE induction in lethally irradiated WT recipient mice adoptively transferred with WT or *Tpl2*-KO BM cells ($n = 5$ mice per group). (B and C) Flow cytometry analysis of CNS-infiltrating mononuclear cells of day 15 MOG_{35-55}-immunized chimeric mice described in A, showing a representative plot (B) and a summary graph (C). $n = 4$ mice per group. (D) Mean clinical scores of age- and sex-matched *Rag1*-KO mice, adoptively transferred with WT and *Tpl2*-KO $CD4^+$ T cells and then subjected to MOG_{35-55}-mediated EAE induction ($n = 5$ mice per group). Data are representative of two independent experiments for all panels. Error bars are mean ± SD values.

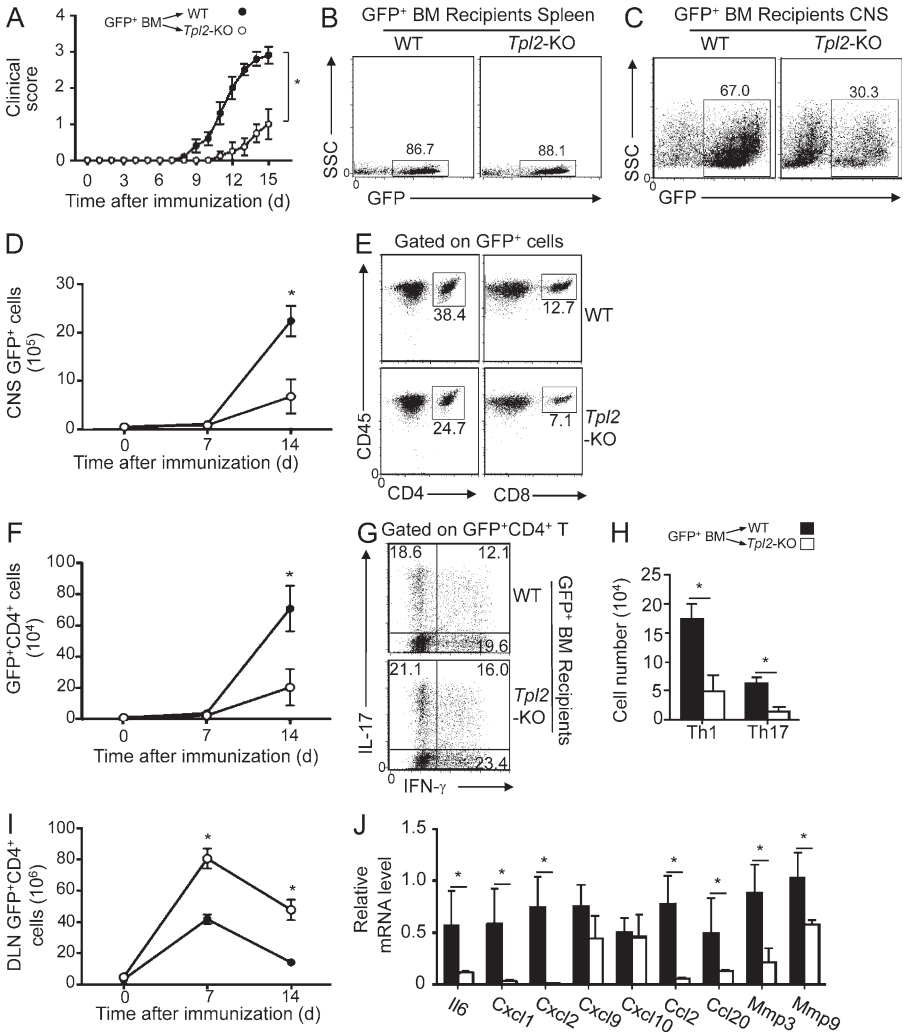

Figure 4. TPL2 deficiency in radioresistant cells inhibits immune cell recruitment into the CNS and ameliorates EAE pathogenesis. (A) Lethally irradiated WT and *Tpl2*-KO mice were adoptively transferred with GFP+ WT bone marrow cells, and the generated chimeric mice were subjected to EAE induction by MOG_{35-55}. Graph represents the clinical scores of WT and *Tpl2*-KO GFP-chimeric mice. (B–F) The WT and *Tpl2*-KO GFP+ bone marrow–chimeric mice were either not immunized (B) or immunized with MOG_{35-55} for EAE induction (for 15 d; C–F). Flow cytometry was performed to monitor the frequency of GFP+ cells in the spleen (B), total CNS-infiltrating cells (GFP+; C and D), and CNS-infiltrating (GFP+CD4+; E and F) CD4+ T cells. Data are presented as representative plots (B, C, and E) or summary graphs (D and F). (G and H) Flow cytometric analyses of the frequency (G) and absolute numbers (H) of IFN-γ– and IL-17–producing CD4+ T cells in the CNS (brain and spinal cord) of MOG_{35-55}-immunized WT and *Tpl2*-KO GFP-chimeric mice ($n = 5$ mice per group, day 15 after immunization). (I) Flow cytometric analyses to measure the number of GFP+CD4+ cells in the draining lymph nodes of MOG_{35-55}-immunized WT and *Tpl2*-KO GFP-chimeric mice. (J) QPCR analyses of the relative mRNA expression level of the indicated proinflammatory genes in the spinal cords of MOG_{35-55}-immunized WT and *Tpl2*-KO GFP-chimeric mice ($n = 4$ mice per group, day 15 after immunization). Data were normalized to a reference gene, *Actb*. *, $P < 0.05$. Data are representative of two independent experiments for all panels. Error bars are mean ± SD values.

In contrast to the CNS, the draining lymph nodes of the *Tpl2*-KO chimeric mice had a drastically increased number of CD4+ T cells (Fig. 4 I). These results suggested that T cells were competently activated in *Tpl2*-KO recipient mice by the MOG antigen, but the activated T cells might not be efficiently recruited to the CNS. Consistently, the CNS of the *Tpl2*-KO chimeric mice had reduced expression of the proinflammatory cytokine IL-6 and several chemokines known to be involved in the recruitment of immune cells (Fig. 4 J). Thus, TPL2 functions in the radio-resistant nonhematopoietic cells to mediate leukocyte infiltration into the CNS and the pathogenesis of EAE.

TPL2 is required for EAE induction by Th17 cells

To further elucidate the mechanism by which TPL2 regulates EAE pathogenesis, we performed passive EAE to specifically address the role of TPL2 in mediating CNS inflammation induced by preactivated $MOG_{35–55}$-specific Th17 cells. When adoptively transferred into the WT recipient mice, both the WT and the *Tpl2*-KO MOG-specific Th17 cells efficiently induced EAE, emphasizing a dispensable role for TPL2 in mediating the cell-intrinsic effector function of Th17 cells (Fig. 5, A and B). In contrast, the *Tpl2*-KO recipients developed very weak EAE clinic scores regardless of whether they were transplanted with the WT or *Tpl2*-KO Th17 cells (Fig. 5, A and B). Parallel flow cytometric analyses revealed that the *Tpl2*-KO recipient mice had a severe defect in mediating Th17 cell–induced immune cell infiltration into the CNS (Fig. 5, C–E). Such a defect was seen with all of the major immune cell populations, including the CD4+ and CD8+ T cells, the CD11b+ monocytes, and the Gr-1+ neutrophils (Fig. 5, C and D). By adoptively transferring MOG-specific Th17 cells derived from the B6.SJL mice (expressing the CD45.1 congenic marker), we found that the *Tpl2*-KO mice were defective in recruiting the transferred T cells to the CNS (Fig. 5 E), causing their accumulation in the spleen (Fig. 5 F).

Th1 cells are also known to induce EAE, although the underlying mechanism is different from that mediating the Th17-triggered EAE (Simmons et al., 2013). To examine whether TPL2 specifically mediates the inflammatory responses to Th17

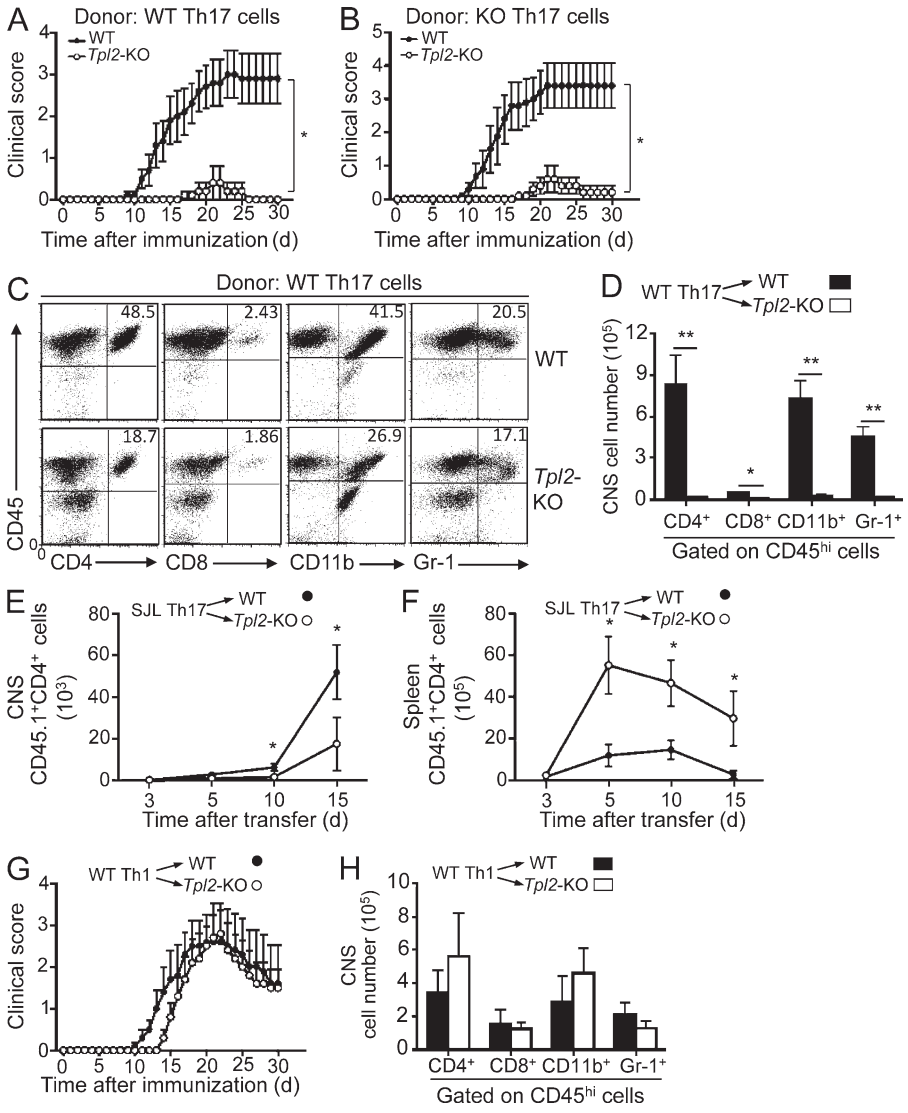

Figure 5. TPL2 is required for EAE induction by Th17 cells but not by Th1 cells. (A and B) EAE clinical scores of WT or *Tpl2*-KO mice adoptively transferred with MOG_{35-55}-specific Th17 T cells (donor) derived from MOG_{35-55}-immunized WT (A) or *Tpl2*-KO (B) mice. (C and D) Flow cytometry analysis of the indicated immune cell ($CD45^+$) populations infiltrated into the CNS (brain and spinal cord) of adoptively transferred WT and *Tpl2*-KO mice described in A ($n = 4$ mice per group, day 15 after donor Th17 cell transfer). Data are presented as a representative plot (C) and summary graphs of the absolute cell numbers (D). (E and F) Absolute cell number of the transferred $CD4^+$ T cells ($CD45.1^+$) in CNS (brain and spinal cord, E) and spleen (F) of WT and *Tpl2*-KO mice adoptively transferred with MOG-specific $CD45.1^+$ Th17 cells (derived from B6.SJL mice), determined by flow cytometry ($n = 4$ mice per group). (G) EAE clinical scores of WT and *Tpl2*-KO mice adoptively transferred with MOG_{35-55}-specific WT Th1 cells. (H) Absolute cell number of the indicated immune cell populations infiltrated into the CNS (brain and spinal cord) of adoptively transferred WT and *Tpl2*-KO mice described in G ($n = 4$ mice per group, day 15 after donor Th1 cell transfer). *, $P < 0.05$; **, $P < 0.01$. Data are representative of three independent experiments. Error bars are mean ± SD values.

cells or also the responses to Th1 cells, we performed passive EAE using MOG-specific Th1 cells. The TPL2 deficiency only weakly delayed the induction of EAE by Th1 cells (Fig. 5 G). Consistently, the adoptively transferred Th1 cells induced similar levels of CNS-infiltrating immune cells in the WT and *Tpl2*-KO recipients (Fig. 5 H). Thus, TPL2 had a predominant role in mediating the Th17 responses.

TPL2 is required for IL-17–stimulated gene expression

IL-17 is a signature cytokine of Th17 cells that stimulates the expression of various chemokines and proinflammatory cytokines in CNS cells, particularly astrocytes (Kang et al., 2010; Zepp et al., 2011). Given the specific role of TPL2 in mediating Th17 cell–induced EAE and the defect of IL-17 target gene induction in the CNS of EAE-induced *Tpl2*-KO mice, we further assessed the involvement of TPL2 in mediating IL-17–dependent EAE pathogenesis by examining the effect of an IL-17 blocking antibody on EAE induction in WT or *Tpl2*-KO mice. For these studies, we used the WT and *Tpl2*-KO chimeric mice reconstituted with WT bone marrow cells. Consistent with the results presented in Fig. 4 A, the *Tpl2*-KO chimeric mice had attenuated EAE induction compared with the WT chimeric mice (Fig. 6 A). More importantly, injection of the IL-17 blocking antibody greatly inhibited EAE severity in WT chimeric mice, but not in *Tpl2*-KO chimeric mice (Fig. 6 A). The findings suggested that the IL-17–stimulated EAE pathogenesis might be already defective in the *Tpl2*-KO chimeric mice and, thus, not further reduced by the IL-17 blocking antibody. Indeed, parallel gene expression analyses revealed that the expression of several known IL-17 target genes, *Cxcl1*, *Cxcl2*, and *Tnf*, although not Cxcl10, in astrocytes was substantially reduced in the *Tpl2*-KO chimeric mice compared with that of the WT chimeric mice during EAE induction (Fig. 6 B). Furthermore, the IL-17 blocking antibody inhibited the astrocyte gene expression in the WT but not the *Tpl2*-KO chimeric mice (Fig. 6 B). Parallel analysis of gene expression in the CNS endothelial cells only revealed some minor effect of anti–IL-17 antibody or TPL2 deficiency on

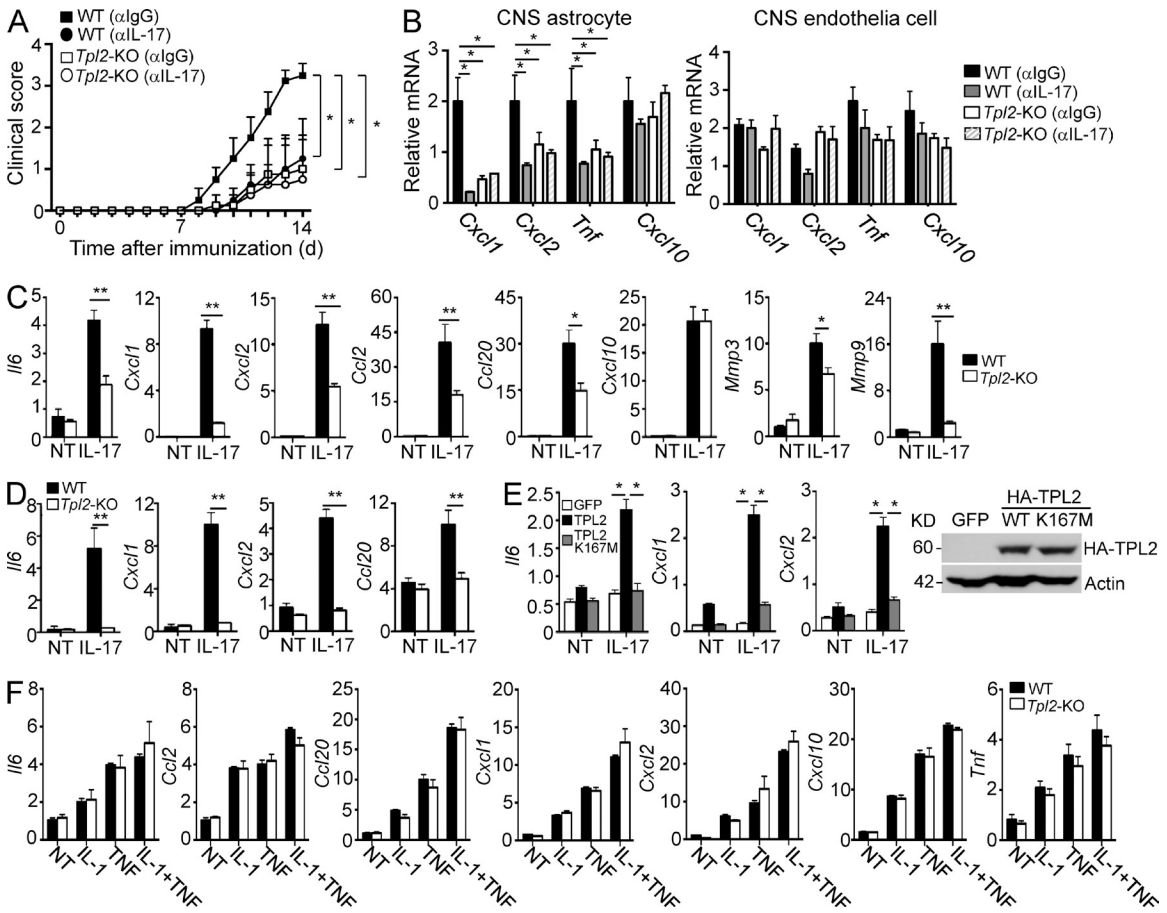

Figure 6. TPL2 mediates IL-17–stimulated gene expression. (A and B) Lethally irradiated WT and *Tpl2*-KO mice were adoptively transferred with WT bone marrow cells derived from B6.SJL mice, and the generated chimeric mice were subjected to EAE induction by MOG_{35-55}. The mice were also intravenously injected with control rabbit IgG or an anti–IL-17 antibody on days 5, 7, 9, and 11 after MOG immunization ($n = 4$ mice per group). The mice were monitored for mean clinical scores (A) and sacrificed on day 14 for QPCR analyses of the indicated genes using FACS-sorted CNS astrocytes ($CD45.1^{-}ASCA\text{-}1^{+}$) or endothelial cells ($CD45.1^{-}CD31^{+}$). (C and D) QPCR analysis of relative mRNA expression for the indicated genes in WT and *Tpl2*-KO astrocytes (C) or primary MEFs (D) that were either not treated (NT) or stimulated with IL-17 for 6 h. Data were normalized to a reference gene, *Actb*. (E) TPL2-deficient primary MEFs were reconstituted by retroviral infection with expression vectors encoding GFP, HA-TPL2, or a catalytically inactive HA-TPL2 mutant (K167M). QPCR was performed for analysis of the relative mRNA levels for the indicated genes, and an IB was performed to monitor TPL2 expression. (F) QPCR analysis of relative mRNA expression for the indicated cytokine and chemokine genes in WT and *Tpl2*-KO astrocytes stimulated with IL-1, TNF, or IL-1 plus TNF for 2 h. *, $P < 0.05$; **, $P < 0.01$. P-values were calculated based on 3 technical repeats, and data are representative of one (A and B), two (F), or at least three (C–E) independent experiments. Error bars are mean ± SD values.

IL-17 target gene expression (Fig. 6 B). These findings are in agreement with a previous report that ablation of the IL-17R adaptor Act1 in astrocytes, but not in endothelial cells, attenuates EAE pathogenesis (Kang et al., 2010).

To more directly examine the role of TPL2 in mediating IL-17–stimulated gene expression, we analyzed the in vitro gene induction by IL-17 in primary astrocytes prepared from unimmunized WT or *Tpl2*-KO mice. Importantly, the TPL2 deficiency severely attenuated the IL-17–stimulated expression of most, although not all, of these genes (Fig. 6 C). The role of TPL2 in mediating IL-17–stimulated gene expression was also seen in MEFs, a cell type which has been frequently used as a model system to study IL-17R signaling (Fig. 6 D). Stable expression of WT TPL2, but not the control protein GFP or a catalytically inactive TPL2 mutant, K167M, restored the IL-17 response in the *Tpl2*-KO MEFs (Fig. 6 E). In contrast to its essential role in IL-17 response, TPL2 was dispensable for gene induction by the inflammatory cytokines TNF and IL-1β (Fig. 6 F). These results establish TPL2 as a pivotal kinase that mediates IL-17–stimulated gene expression and EAE pathogenesis.

TPL2 mediates IL-17–stimulated activation of multiple pathways but is dispensable for ERK activation

TPL2 is known as a kinase that selectively mediates the activation of ERK by TLRs (Dumitru et al., 2000). Our finding that TPL2 mediates IL-17–stimulated gene expression raised the question of how TPL2 regulates IL-17R signaling. We addressed this question using both primary astrocytes and primary MEFs. To our surprise, TPL2 was dispensable for IL-17–stimulated

ERK phosphorylation in both astrocytes (Fig. 7 A) and MEFs (Fig. 7 B). In contrast, TPL2 deficiency severely attenuated the IL-17–stimulated activation of JNK and p38 (Fig. 7, A and B). Moreover, the loss of TPL2 also reduced the phosphorylation of the IKK target protein, IκBα, in astrocytes and MEFs (Fig. 7, A and B). The phosphorylation of two other IKK target proteins, p65 and p105, was also partially inhibited in the *Tpl2*-KO cells (Fig. 7, A and B). Consistently, the TPL2 deficiency strongly inhibited, although did not completely block, the activation of IKK (Fig. 7, C and D) and NF-κB (Fig. 7 E). These signaling defects of the TPL2-deficient cells were not due to reduced expression of IL-17R or the signaling adaptor ACT1 (Fig. 7, F and G). Thus, in contrast to its ERK-specific regulatory role in the TLR pathway, TPL2 is dispensable for ERK activation but is involved in the activation of IKK, JNK, and p38 in the IL-17 signaling pathway. Parallel studies revealed that TPL2 deficiency did not appreciably affect IL-1–stimulated phosphorylation of JNK, p38, IKK, or their upstream regulator TAK1 but substantially reduced the phosphorylation of ERK (Fig. 7 H). These data further suggest that TPL2 has a novel signaling function in the IL-17R pathway.

TPL2 is a pivotal mediator of TAK1 activation by IL-17

A major signaling molecule recruited to the IL-17R is TAK1, which mediates IL-17–stimulated activation of IKK/NF-κB but not ERK (Qian et al., 2007; Zhu et al., 2012). However, the mechanism by which TAK1 is activated by IL-17R signaling is largely unclear. The important role of TPL2 in mediating IL-17R signaling prompted us to examine the role of TPL2 in TAK1 regulation. Consistent with the requirement for TAK1 in mediating IL-17R signaling, we found that IL-17 stimulated the activation of TAK1 in both astrocytes and MEFs, as revealed through detection of TAK1 activation-loop phosphorylation (Fig. 8, A and B) and in vitro TAK1 kinase assays (Fig. 8 C). More importantly, the TPL2 deficiency severely crippled the activation of TAK1 (Fig. 8, A–C). These

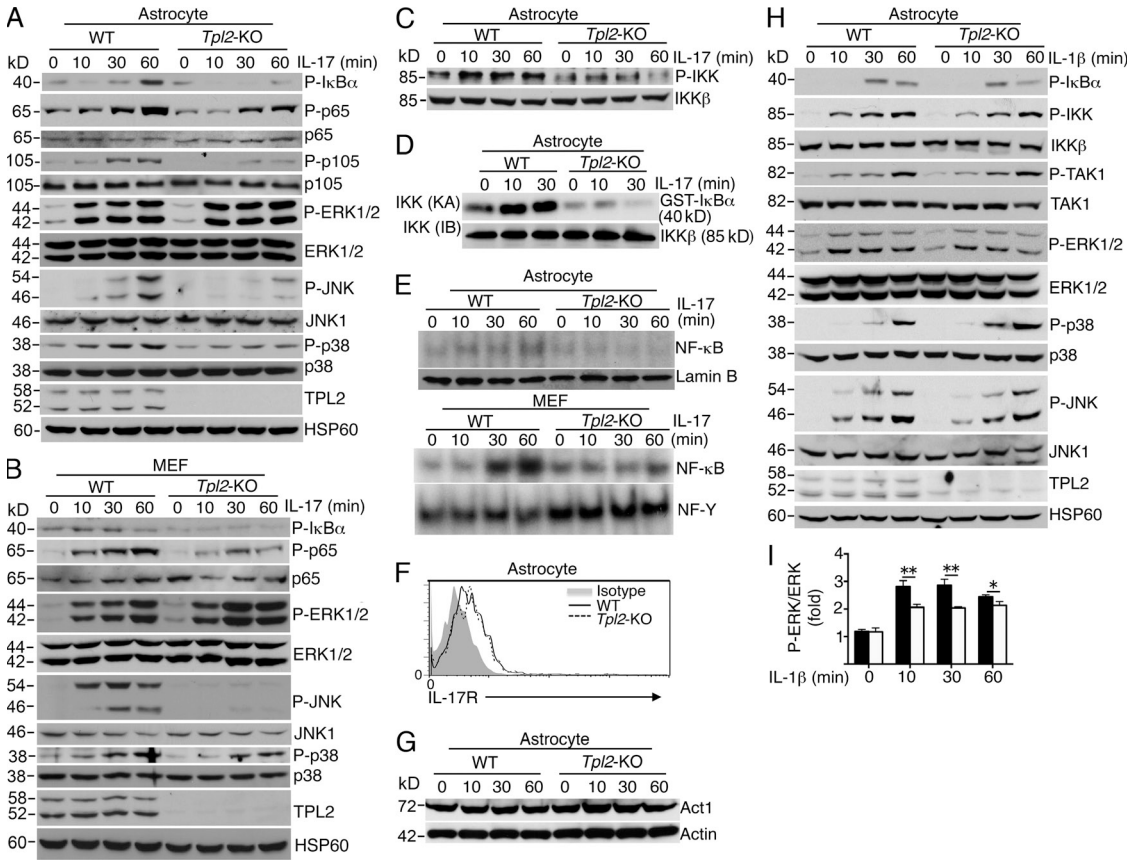

Figure 7. TPL2 mediates IL-17–stimulated activation of multiple signaling pathways. (A and B) IB analyses of the indicated phosphorylated (P-) and total proteins in lysates from WT and *Tpl2*-KO astrocytes (A) or MEFs (B) stimulated for the indicated time periods with 100 ng/ml IL-17. (C) IB analysis of phosphorylated (P-) IKK and total IKKβ in IL-17-stimulated astrocytes. (D) IKK complex was isolated from WT and *Tpl2*-KO astrocyte by IP (using anti-IKKγ) and subjected to IKK kinase assay (KA) using 1 µg GST-IκBα (1–54) as a substrate or IKKβ IB (IB) assay. (E) WT and *Tpl2*-KO astrocyte and MEFs were stimulated with 100 ng/ml IL-17 for the indicated time periods, and nuclear extracts were subjected to NF-κB EMSAs. A Lamin B IB and an NF-Y EMSA were used as loading controls. (F) Flow cytometry analysis of IL-17R expression on WT and *Tpl2*-KO primary astrocytes. (G) IB analysis of the Act1 in the lysates of *Tpl2*-KO and WT control astrocyte stimulated with IL-17 for the indicated time periods. (H) IB analyses of the indicated phosphorylated (P-) and total proteins in lysates from WT and *Tpl2*-KO astrocytes stimulated for the indicated time periods with 20 ng/ml IL-1β. (I) P-ERK and total ERK bands in H were quantified by densitometry. Data are representative of two (F–H) or at least three (A–E) independent experiments. *, $P < 0.05$; **, $P < 0.01$. Error bars are mean ± SD values.

findings establish TPL2 as a crucial mediator of TAK1 activation in the IL-17R signaling pathway.

To determine whether TPL2 serves as a direct kinase of TAK1, we performed TPL2 in vitro kinase assays using a GST-TAK1 fusion protein containing the kinase domain (amino acids 1–292) of a catalytically inactive TAK1 mutant (K63R). Indeed, immunoprecipitated TPL2 potently phosphorylated TAK1, and this kinase activity of TPL2 was stimulated by IL-17 (Fig. 8 D). A purified recombinant TPL2 also phosphorylated the GST-TAK1 substrate (Fig. 8 E). Using *Tpl2*-KO MEFs reconstituted with WT TPL2 or its catalytically inactive mutant (K167M), we further demonstrated that the WT TPL2, but not catalytically inactive TPL2, mediates TAK1 phosphorylation (Fig. 8 F). Thus, TPL2 responds to the IL-17R signal and serves as an upstream kinase of TAK1.

TPL2 physically interacts with TAK1 in response to IL-17 stimulation

We next examined whether TPL2 could physically interact with TAK1. TPL2 was not bound by TAK1 in unstimulated cells, but these two proteins physically associated to form a stable complex in response to IL-17 stimulation (Fig. 8 G). Previous studies demonstrate that TPL2 is stably associated with an inhibitory protein, NF-κB1 p105, which blocks the binding of TPL2 to its downstream target MEK1 in TLR pathway (Beinke et al., 2003, 2004; Waterfield et al., 2003, 2004). TLR signal stimulates the liberation of TPL2 from p105 via IKK-mediated p105 phosphorylation and degradation, thereby allowing TPL2 to phosphorylate MEK1 (Beinke et al., 2003, 2004; Waterfield et al., 2003, 2004). Interestingly, we found that IL-17 also stimulated the release of TPL2 from

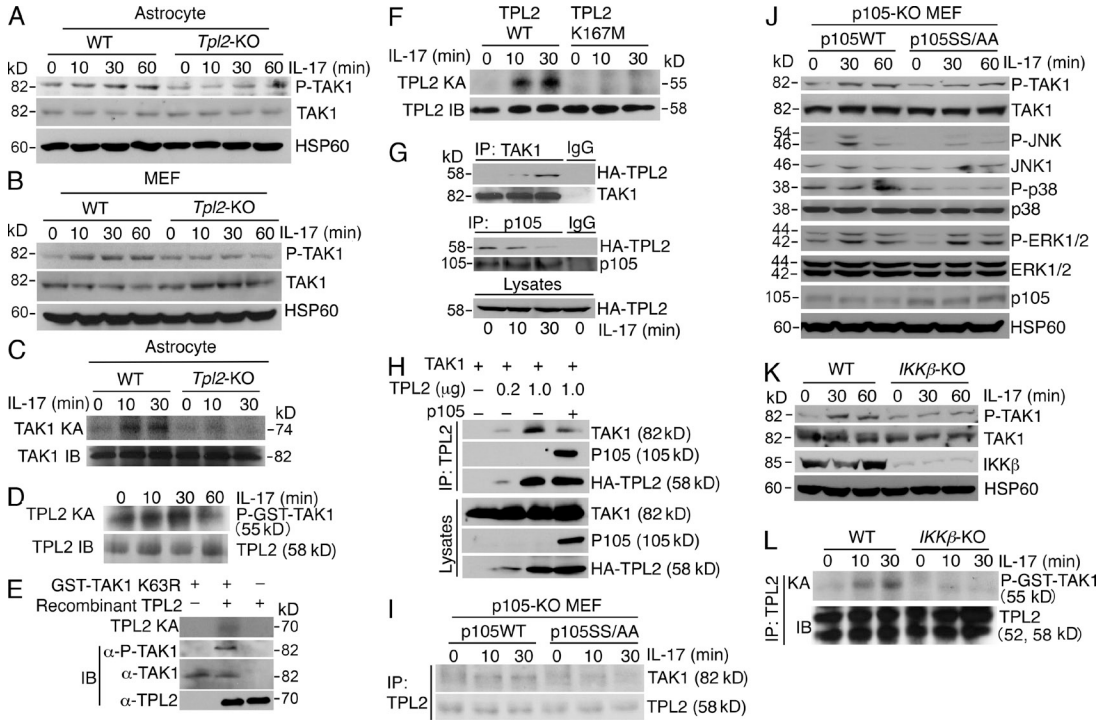

Figure 8. TPL2 phosphorylates TAK1 and mediates IL-17–stimulated TAK1 activation. (A and B) IB analysis of phosphorylated (P-) and total TAK1, as well as the loading control HSP60, in lysates of WT and *Tpl2*-KO astrocytes (A) and MEFs (B), stimulated for the indicated time periods with 100 ng/ml IL-17). (C) TAK1 was isolated by IP from IL-17–stimulated WT and *Tpl2*-KO astrocytes and subjected to kinase assay (KA) using GST-MKK7 (1 μg) as substrate. The KA membrane was analyzed by IB to monitor TAK1 protein level. (D–F) TPL2 in vitro kinase assays using TPL2 isolated (by IP) from IL-17–stimulated astrocytes (D) or *Tpl2*-KO MEFs reconstituted with WT or K167M mutant of TPL2 (F) or using purified recombinant TPL2 (E). 1 μg GST-TAK1-K63R-V5-(1–292) (labeled GST-TAK1) was used as kinase assay substrate. The phosho-TAK1 (Thr187) antibody (α–P-TAK1) was used for phospho-IB (E). (G) HA-TPL2–reconstituted *Tpl2*-KO MEFs were stimulated with IL-17 (100 ng/ml) and subjected to the indicated IP assays, followed by detecting precipitated and coprecipitated proteins (labels on the right) by IB. (H) 293T cells were transfected with the expression vectors indicated on top of the figure. Whole-cell lysates were subjected to IP using anti-TPL2, followed by IB analysis of the precipitated and coprecipitated proteins. Lysates were also analyzed by direct IB. (I) IB of TAK1 and TPL2 in the TPL2 complex isolated by IP from IL-17–stimulated p105-KO MEFs reconstituted with WT or a degradation-resistant mutant (SS/AA) of p105. (J) p105-KO MEFs were reconstituted with WT p105 or a p105 mutant harboring serine to alanine substitutions at its phosphorylation site. The cells were stimulated with 100 ng/ml IL-17 for the indicated time periods, and whole-cell lysates were subjected to IB analysis of the indicated phosphorylated (P-) and total. (K) IB analysis of phosphorylated (P-) and total TAK1 in the lysates of *IKKβ*-KO and WT control MEFs stimulated with IL-17 for the indicated time periods. (L) A TPL2 kinase assay (KA) in IL-17–stimulated *IKKβ*-KO and WT control MEFs. The TPL2 KA membrane was subsequently subjected to IB using HRP-conjugated anti-TPL2. Data are representative of two (A–C, F, and G) or at least three (D, E, H, and I) independent experiments.

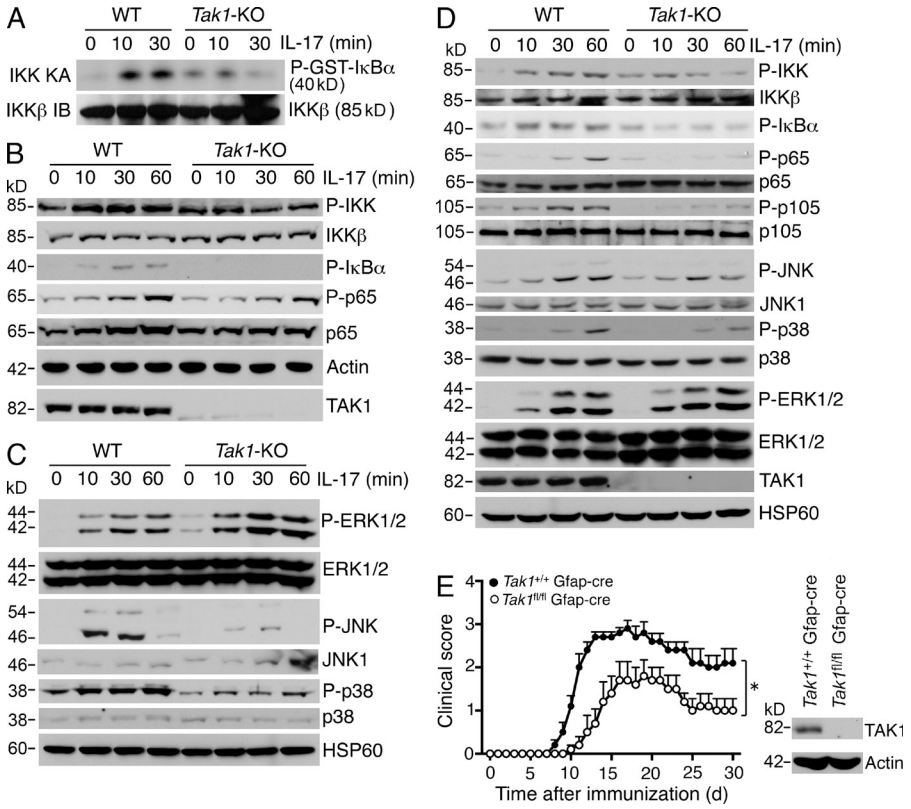

Figure 9. TAK1 mediates IL-17–induced activation of JNK, p38, and IKK/NF-κB. (A) IKK was isolated by IP (using anti-IKKγ) from whole-cell lysates of IL-17–stimulated WT or *Tak1*-KO MEFs and subjected to kinase assays (KA) using 1 µg GST-IκBα (1–54) as a substrate, followed by IKKβ IB. (B) IB analysis of the indicated phosphorylated (P-) and total proteins in the whole-cell lysates from WT and *Tak1*-KO MEFs. (C) IB analysis of the indicated phosphorylated (P-) and total proteins in the whole-cell lysates from WT and *Tak1*-KO MEFs. (D) IB analyses of the indicated phosphorylated (P-) and total proteins in whole-cell lysates from WT and *Tak1*-KO primary astrocytes stimulated with 100 ng/ml IL-17. (E) Mean clinical scores of age- and sex-matched *Tak1*$^{+/+}$Gfap-cre and *Tak1*$^{fl/fl}$Gfap-cre mice subjected to MOG_{35-55}-induced EAE ($n = 5$ mice per group). An IB, using astrocytes of unimmunized mice, was included to show the efficiency of TAK1 ablation. Data are representative of three independent experiments for all panels. *, $P < 0.05$. Error bars are mean ± SD values.

p105, which is coupled with TPL2–TAK1 interaction (Fig. 8 G, middle). Conversely, overexpressed TPL2 bound to TAK1, and this physical interaction was inhibited upon expression of p105 (Fig. 8 H). Furthermore, the IL-17–stimulated TPL2/TAK1 binding (Fig. 8 I), as well as the phosphorylation of TAK1 and its downstream targets, JNK and p38 (Fig. 8 J), were inhibited in p105-deficient MEF cells reconstituted with a degradation-resistant p105 mutant lacking its phosphorylation site (p105SS/AA). Consistent with these findings, the IL-17–stimulated TAK1 phosphorylation and kinase activity were severely attenuated in MEFs lacking IKKβ (Fig. 8, K and L). Collectively, these results suggest that the TPL2-mediated activation of TAK1 in the IL-17R pathway involves TPL2–TAK1 physical interaction, which in turn requires IKK-mediated p105 phosphorylation and TPL2 liberation from p105.

TAK1 is required for activation of IKK, JNK, and p38 by IL-17 and for EAE pathogenesis

Although TAK1 is known as a mediator of IL-17–stimulated IKK/NF-κB activation, its precise signaling function in the IL-17 pathway has not been thoroughly analyzed using genetic approaches. To better understand the function of TAK1 in mediating IL-17R signaling and further confirm the functional significance of the TPL2–TAK1 connection, we analyzed the effect of TAK1 deficiency on the activation of various downstream pathways using TAK1-deficient cells. Consistent with prior gene knockdown studies in HeLa cells (Zhu et al., 2012), we found that the TAK1-deficient MEFs had reduced activation of IKK by IL-17 (Fig. 9 A). The IL-17–stimulated phosphorylation– of IKK and its downstream targets, IκBα and p65, was also inhibited to different extents in these mutant MEFs (Fig. 9 B). Our finding that TPL2 was required for activation of both TAK1 and the MAPKs (JNK and p38) raised the intriguing question of whether TAK1 was important for JNK/p38 activation in the IL-17 pathway. We found that the TAK1 deficiency in MEFs indeed attenuated the IL-17–stimulated phosphorylation of both JNK and p38 (Fig. 9 C). In contrast, TAK1 was dispensable for the activation of ERK. To examine the role of TAK1 in mediating IL-17 signaling in astrocytes, we prepared primary WT and *Tak1*-KO astrocytes using an inducible knockout system. We crossed the TAK1-floxed mice with CreER mice to generate TAK1$^{+/+}$CreER and *TAK1*$^{fl/fl}$CreER mice. We prepared astrocytes from the newborn TAK1$^{+/+}$CreER and *TAK1*$^{fl/fl}$CreER mice and then incubated them with tamoxifen to produce the WT and *Tak1*-KO astrocytes, respectively. Consistent with the results obtained with MEFs, the TAK1 deficiency in astrocytes attenuated, although did not completely block, the IL-17–stimulated phosphorylation of IKK as well as JNK and p38, but not the phosphorylation of ERK (Fig. 9 D). These results were consistent with the requirement of TPL2 for IL-17–stimulated activation of IKK/NF-κB, JNK, and p38 (Fig. 7, A and B), thus further emphasizing the role of TPL2 in mediating the TAK1 axis of IL-17R signaling.

To examine the in vivo role of TAK1 in regulating EAE induction, we generated astrocyte-specific *Tak1*-KO mice by crossing the *Tak1*-floxed mice with mice expressing Cre recombinase under the control of the astrocyte-specific glial

fibrillary acidic protein (Gfap) promoter (Gfab-Cre; Garcia et al., 2004; Spence et al., 2011). As seen with the *Tpl2*-KO mice, the *Tak1*$^{fl/fl}$Gfap-Cre mice displayed delayed onset and reduced severity of EAE compared with the control *Tak1*$^{+/+}$ Gfap-Cre mice (Fig. 9 E).

DISCUSSION

The molecular mechanism mediating the pathogenesis of MS and its animal model, EAE, remains poorly understood. In this study, we have identified TPL2 as a crucial signaling factor mediating CNS inflammation and the pathogenesis of EAE. We show that TPL2 is dispensable for activation of inflammatory T cells, but it is required for the inflammatory effector function of Th17 cells within the CNS. Our data suggest that TPL2 is particularly important for IL-17–stimulated expression of chemokines and proinflammatory cytokines in astrocytes, a cell type known to be crucial for Th17 cell–stimulated CNS inflammation (Kang et al., 2010). Interestingly, TPL2 serves as a master kinase that mediates IL-17–stimulated activation of several signaling pathways, including those leading to the activation of IKK/NF-κB, JNK, and p38. We have obtained genetic and biochemical evidence that TPL2 acts by connecting the IL-17R signal to the activation of TAK1. In response to IL-17 stimulation, TPL2 physically associates with TAK1 and mediates the phosphorylation and catalytic activation of TAK1. Thus, our data suggest that TPL2 is an essential upstream kinase of TAK1 in the IL-17R signaling pathway.

Due to the involvement of IL-17 in various autoimmune and inflammatory disorders, IL-17R signaling has become a hot topic of study during recent years (Gaffen, 2009; Zepp et al., 2011; Song and Qian, 2013). Important progress has been made to understand the IL-17R proximal signaling events. Analogous to the TLRs, the IL-17R signals through the recruitment of an adaptor molecule, ACT1, and utilizes TRAF members, particularly TRAF6. IL-17R also resembles TLRs in the stimulation of multiple downstream pathways, including NF-κB, C/EBP, and the three families of MAPKs: JNK, p38, and ERK. Despite the extensive studies on ACT1, how exactly the downstream pathways are linked to IL-17R–proximal signal is still poorly understood. Using a genetic approach, we showed in this study that the kinase TAK1 is important for IL-17–stimulated activation of two major MAPKs (JNK and p38) in addition to its known role in the regulation of IKK/NF-κB activation. This finding explains the crucial role for TAK1 in mediating the gene induction by IL-17 (Qian et al., 2007). Our finding that TPL2 mediates TAK1 activation by the IL-17R and the pathological effector functions of Th17 cells in the CNS provides additional novel insights into the mechanism of IL-17R signaling.

The signaling function of TPL2 has thus far been studied mainly in the TLR pathways using macrophages and dendritic cells (Gantke et al., 2011). It is generally thought that TPL2 promotes inflammation by mediating the posttranslational induction of TNF secretion (Dumitru et al., 2000). Our finding that TPL2 mediates the TAK1 axis of IL-17R signaling highlights a novel signaling mechanism of TPL2 function in inflammation. We found that TPL2 functions in CNS-resident cells, including astrocytes, to regulate the pathogenesis of EAE. Given the important role of IL-17 in different inflammatory processes, it is likely that TPL2 may be involved in additional autoimmune diseases. Recent studies suggest that TPL2 also plays a role in regulating the differentiation of CD4$^+$ T cells (Sugimoto et al., 2004; Watford et al., 2008). Consistent with a prior study (Watford et al., 2008), we found that the TPL2-deficient naive CD4$^+$ T cells produced reduced levels of Th1 cells when differentiated in vitro. Interestingly, however, TPL2 was completely dispensable for Th1 induction in vivo during the course of EAE. In fact, we consistently detected a higher level of Th1 cells in the peripheral lymphoid organs of the *Tpl2*-KO mice after EAE induction, which is probably due to the attenuated recruitment of effector T cells from the peripheral lymphoid organs to the CNS. TPL2 has also been implicated in the regulation of T reg cells (Serebrennikova et al., 2012). Our current study did not detect a major effect of TPL2 deficiency on T reg cell production. This discrepancy is likely due to the different conditions used in the in vitro T reg cell differentiation assays. Nevertheless, the TPL2 deficiency also did not affect T reg generation in vivo during EAE induction. Using the passive EAE approach, we found that TPL2 is also dispensable for the effector function of Th1 cells. Our data suggest that TPL2 plays a crucial role in mediating CNS inflammation and EAE pathogenesis induced by the Th17 subset of inflammatory T cells.

TPL2 is best known as a kinase that mediates activation of the MEK1–ERK signaling pathway by TLRs (Gantke et al., 2011; Vougioukalaki et al., 2011). TPL2 ablation largely blocks the TLR-stimulated activation of ERK without affecting the activation of JNK, p38, or IKK/NF-κB (Dumitru et al., 2000). Interestingly, despite the common downstream pathways shared by the TLRs and IL-17R, we found that TPL2 is completely dispensable for ERK activation by the IL-17R, thus suggesting fundamental differences in the signal transduction mediated by the TLRs and IL-17R. Although the precise underlying mechanism warrants further studies, it seems clear that TPL2 targets two different kinases, MEK1/2 and TAK1, in the TLR and IL-17R pathways. Although MEK1/2 is an essential upstream activator of ERK, our genetic evidence suggests that TAK1 is dispensable for ERK activation. Instead, TAK1 mediates the activation of IKK, JNK, and p38, explaining the crucial role of TPL2 in regulating these downstream kinases in the IL-17R pathway.

Previous work from others and us reveals that the signaling function of TPL2 is regulated by the NF-κB1 precursor protein p105 (Beinke et al., 2003; Waterfield et al., 2003). TPL2 forms a stable complex with p105, in which p105 both stabilizes TPL2 and prevents the access of TPL2 to its substrate protein MEK1/2. TLR-stimulated MEK1/2 activation requires IKKβ-mediated phosphorylation and degradation of p105 and also involves IKKβ-mediated TPL2 phosphorylation (Beinke and Ley, 2004; Waterfield et al., 2004; Roget et al., 2012). Our data suggest that the TPL2–TAK1 physical interaction is also inhibited by p105. IL-17 stimulates the dissociation

of TPL2 from p105, which is coupled with the association of TPL2 with TAK1 and the activation of the TAK1-specific TPL2 kinase activity. Consistently, we found that IKKβ is required for IL-17–stimulated activation of TAK1 and its downstream kinases in MEFs. We also obtained similar results using astrocytes treated with a selective IKKβ inhibitor, PS1145 (unpublished data). These findings suggest that IKK plays a crucial role in the initiation and positive-feedback regulation of the TPL2–TAK1 signaling axis in the IL-17R signaling pathway.

How can IKK serve as both a target and a regulator of the TPL2–TAK1 signaling axis? We found that the TPL2 deficiency does not completely block the IL-17–stimulated activation of IKK and phosphorylation of p105. This suggests that the IKK activated through a TPL2-independent pathway mediates the initial activation of the TPL2–TAK1 signaling axis. Once activated, this axis targets the activation of not only p38 and JNK but also IKK, leading to a positive-feedback loop. We noticed that the inhibitory effect of TPL2 deficiency on IL-17–stimulated IκBα phosphorylation and NF-κB activation seems to be more profound than that on the phosphorylation of p65 and p105. This phenotype may be explained by a recent study suggesting differences in IKK-mediated phosphorylation of distinct substrates (Schröfelbauer et al., 2012). The phosphorylation of IκBα is more stringently controlled and requires IKKγ, whereas the phosphorylation of p105 and p65 is independent of IKKγ. Although the underlying mechanism is complex and needs further studies, our current finding supports a positive-feedback model of TPL2–TAK1 activation.

MATERIALS AND METHODS

Mice. The *Tpl2*-KO mice (on C57BL/6 background) were provided by P.N. Tsichlis (Tufts University, Medford, MA; Dumitru et al., 2000). The $Tpl2^{+/-}$ heterozygous mice were bred to generate age-matched $Tpl2^{-/-}$ (*Tpl2*-KO) and $Tpl2^{+/+}$ (WT) mice. The *Tak1*-floxed mice (C57BL/6 and 129/Sv mixed background; provided by S. Akira, Osaka University, Osaka, Japan; Sato et al., 2005) were crossed with B6.129-Gt(ROSA)26Sortm1(cre/ERT2)Tyj/J (called CreER in this study) mice (C57BL/6 background; The Jackson Laboratory) or with B6.Cg-Tg(Gfap-cre)73.12Mvs/J mice (C57BL/6 background; The Jackson Laboratory; called Gfap-Cre in this study). The B6.SJL mice (expressing the CD45.1 congenic marker) and GFP transgenic (C57BL/6-Tg(CAG-EGFP)10sb/J) mice were obtained from The Jackson Laboratory. The mice were maintained in a specific pathogen-free facility, and the animal experiments were performed in accordance with protocols approved by the Institutional Animal Care and Use Committee of the University of Texas MD Anderson Cancer Center.

Plasmids, antibodies, and reagents. The pcDNA-HA-TPL2, pCLXSN-HA-TPL2, and pCLXSN-HA-TPL2 K167M (catalytically inactive mutant) plasmid vectors have been previously described (Waterfield et al., 2003; Babu et al., 2006). The pCMV4-HA-TAK1 expression vector was provided by K. Matsumoto (Nagoya University, Nagoya, Japan; Shibuya et al., 1996). GST-IκBα (1–54) was constructed by inserting a DNA fragment encoding the N-terminal 54 amino acids of human IκBα into the pGEX-4T-3 vector. This vector was used to prepare GST-IκBα (1–54) recombinant protein in bacteria. The GST-MKK6 and GST-MKK7 recombinant proteins were purchased from Millipore, and the GST-TAK1-K63R-V5-(1–292) recombinant protein (a catalytically inactive TAK1 kinase domain harboring a site mutation in its ATP-binding site) was provided by J. Yang (Baylor College of Medicine, Houston, TX). Murine IL-17 (IL-17A) recombinant protein was obtained from R&D Systems, and the IKKβ inhibitor PS1145 was from Sigma-Aldrich.

The HRP-conjugated anti-HA (3F10) antibody was purchased from Roche. Anti-p105 (C-19), anti-ERK (K-23), anti–phospho-ERK (E-4), anti-JNK (C-17), anti-p38 (H-147), anti-TPL2 (anti-Cot M20, regular and HRP-conjugated), anti-HSP60 (H-1), anti–Lamin B (C-20), IL-17R (H-168), and Act1 (H-300) were obtained from Santa Cruz Biotechnology, Inc. Antibodies for IKKβ, phospho-IKK (IKKα [Ser176]/IKKβ [Ser177]), phospho-TAK1 (Thr187), phospho-IκBα (Ser32), phospho-JNK (Thr180/Tyr185), phospho-p38 (Thr180/Tyr182), and phospho-p65 (Ser536) were purchased from Cell Signaling Technology. Anti-TAK1 was provided by J. Ninomiya-Tsuji (North Carolina State University, Raleigh, NC), and anti-p65 was from National Cancer Institute Preclinical Repository. Antibodies used for flow cytometry were obtained from eBioscience.

Induction and assessment of EAE. Active EAE was induced essentially as previously described except for not including the repeated immunization (Jin et al., 2009). For passive EAE, we prepared MOG_{35-55}-primed T cells from the spleen and draining LNs of MOG_{35-55}-immunized mice (on day 10) and restimulated the cells in vitro for 5 d with MOG_{35-55} in the presence of IL-23 (for generating Th17 cells) or IL-12 plus anti–IL-23p19 (for generating Th1 cells). The MOG-specific Th1 and Th17 cells (10^7/mouse) were adoptively transferred into sublethally irradiated (500 rad) WT and *Tpl2*-KO mice. The disease severity was scored blindly by a trained observer without knowing the genotype of the mice or treatment protocols by using the standard scale (Jin et al., 2009). We excluded mouse data after the mice reached a score of 5 (moribund state or death). The EAE scores were assessed without group allocation information.

Bone marrow chimeras. Bone marrow cells were prepared from GFP transgenic mice and adoptively transferred into lethally irradiated (950 rad)

Table 1. The specific primers used for real-time PCR

Gene	Forward primer (5′–3′)	Reverse primer (5′–3′)
CCL2	GGGATCATCTTGCTGGTGAA	AGGTCCCTGTCATGCTTCTG
CCL20	TGTACGAGAGGCAACAGTCG	TCTGCTCTTCCTTGCTTTGG
CXCL1	CTTGACCCTGAAGCTCCCTT	AGGTGCCATCAGAGCAGTCT
CXCL2	AAAGTTTGCCTTGACCCTGA	TCCAGGTCAGTTAGCCTTGC
CXCL9	TAGGCAGGTTTGATCTCCGT	CGATCCACTACAAATCCCTCA
CXCL10	CCTATGGCCCTCATTCTCAC	CTCATCCTGCTGGGTCTGAG
IL-6	CACAGAGGATACCACTCCCAACA	TCCACGATTTCCCAGAGAACA
MMP3	AGCCTTGGCTGAGTGGTAGA	CGATGATGAACGATGGACAG
MMP9	CTGTCGGCTGTGGTTCAGT	AGACGACATAGACGGCATCC
Tpl2	TCAGCTTCCAAGGAACAAGG	TCGACCACAAGAATGTGGAA
β-Actin	CGTGAAAAGATGACCCAGATCA	CACAGCCTGGATGGCTACGT

WT or *Tpl2*-KO mice (8 wk old; 10×10^6 per mouse). The lethal-dose irradiation would eliminate the bone marrow and peripheral immune cells without affecting the radioresistant CNS-resident cells, and the bone marrow chimeric mice would thus have their peripheral immune system reconstituted with GFP^+ cells. After 8 wk, the chimeric mice were immunized for EAE induction.

Flow cytometric and histological analyses. Cell suspensions were prepared from the spleens and lymph nodes and subjected to flow cytometric analyses using an LSRII flow cytometer (BD; Reiley et al., 2006). Histological analyses were conducted as described previously (Xiao et al., 2013).

Cell culture. Human embryonic kidney cell line 293T was cultured in DMEM media containing 5% FBS and transfected in 6-well plates using the calcium phosphate method. To prepare *Tpl2*-KO and WT control primary MEFs, $Tpl2^{+/-}$ mice were bred to produce $Tpl2^{+/+}$ (WT) and $Tpl2^{-/-}$ (KO) embryos. MEF cells were prepared from 13.5-d-old embryos dissected from the same pregnant females and were cultured in DMEM medium supplemented with 10% FBS. *IKKβ*-KO and their WT-control MEFs were provided by M. Karin (University of California, San Diego, La Jolla, CA). The *Tak1*-KO mice and their WT control MEFs were provided by S. Akira (Osaka University, Osaka, Japan; Sato et al., 2005).

Mononuclear cells were isolated from the brains and spinal cords of untreated or MOG_{35-55}-immunized mice and subjected to flow cytometric analysis of the different populations of immune cells (Xiao et al., 2013). Primary neuronal cells were isolated from the brains of newborn mice, separated into different populations, and then cultured in vitro as described previously (Xiao et al., 2013). The purity of the astrocytes was >90% as assessed based on staining with an antibody for GFAP (Santa Cruz Biotechnology, Inc.).

In vitro $CD4^+$ T cell differentiation. Purified naive $CD4^+$ T cells ($CD44^{lo}CD62L^{hi}$) were activated with 5 µg/ml of plate-bound anti-CD3 and 1 µg/ml anti-CD28 under Th0 (5 µg/ml anti–IL-4 and 5 µg/ml anti–IFN-γ), Th1 (5 µg/ml anti–IL-4 and 10 ng/ml IL-12), Th17 (5 µg/ml anti–IL-4, 5 µg/ml anti–IFN-γ, 20 ng/ml IL-6, and 2.5 ng/ml TGF-β), or T reg cells (5 µg/ml anti–IL-4, 5 µg/ml anti–IFN-γ, and 1 ng/ml TGF-β) conditions. After 4 d of activation, the differentiated T cells were stained with Foxp3 to quantify the frequency of T reg cells, or restimulated for 4 h with PMA and ionomycin in the presence of the protein transport inhibitor monensin, followed by intracellular staining of IFN-γ and IL-17 to quantify the frequency of Th1 and Th17 cells.

Quantitative RT-PCR (QPCR. Real-time QPCR was performed as previously described (Chang et al., 2009) using gene-specific primer sets (Table 1). The relative mRNA levels were assessed (in triplicate) based upon normalization using a reference gene encoding β-Actin (*Actb*). The fold of induction was calculated relative to the untreated WT sample, which was normalized to the value of 1.

Immunoblot (IB), immunoprecipitation (IP), ubiquitination assays, in vitro kinase assays, and EMSA. The procedures for these assays were performed as described previously (Chang et al., 2009).

Statistical analysis. One-way ANOVA, where applicable, was performed to determine whether an overall statistically significant change existed, followed by the Student's *t* test to analyze the differences between any two groups. Data are presented as means ± SD. A p-value <0.05 is considered statistically significant. In our animal studies, 4 mice are required for each group based on our calculation to achieve a 2.3-fold change (effect size) in two-tailed Student's *t* test with 90% power and a significance level of 5%. All statistical tests justified as appropriate, and the data meet the assumptions of the tests. The variance is similar between the groups that are being statistically compared.

We would like to thank P. Tsichlis and S. Akira for mutant mice, S. Akira and M. Karin for MEF cells, K. Matsumoto for the TAK1 expression vector, J. Yang for the GST-TAK1 recombinant protein, J. Ninomiya-Tsuji for the TAK1 antibody, and the National Cancer Institute Preclinical Repository for the p65 antibody. We also thank the personnel from the National Institutes of Health/National Cancer Institute–supported resources (flow cytometry, DNA analysis, histology, and animal facilities) under award number P30CA016672 at The MD Anderson Cancer Center.

This study was supported by grants from the National Institutes of Health (AI057555, AI064639, GM84459, and AI104519) and partially supported by a seed fund from the Center for Inflammation and Cancer at the MD Anderson Cancer Center.

The authors declare no competing financial interests.

Author contributions: Y. Xiao designed and performed the research, prepared the figures, and wrote part of the manuscript; J. Jin, M. Chang, M. Nakaya, H. Hu, Q. Zou, X. Zhou., G.C. Brittain, and X. Cheng contributed experiments; and S.-C. Sun supervised the work and wrote the manuscript.

Submitted: 19 December 2013
Accepted: 2 June 2014

REFERENCES

Babu, G., M. Waterfield, M. Chang, X. Wu, and S.-C. Sun. 2006. Deregulated activation of oncoprotein kinase Tpl2/Cot in HTLV-I-transformed T cells. *J. Biol. Chem.* 281:14041–14047. http://dx.doi.org/10.1074/jbc.M512375200

Beinke, S., and S.C. Ley. 2004. Functions of NF-κB1 and NF-κB2 in immune cell biology. *Biochem. J.* 382:393–409. http://dx.doi.org/10.1042/BJ20040544

Beinke, S., J. Deka, V. Lang, M.P. Belich, P.A. Walker, S. Howell, S.J. Smerdon, S.J. Gamblin, and S.C. Ley. 2003. NF-κB1 p105 negatively regulates TPL-2 MEK kinase activity. *Mol. Cell. Biol.* 23:4739–4752. http://dx.doi.org/10.1128/MCB.23.14.4739-4752.2003

Beinke, S., M.J. Robinson, M. Hugunin, and S.C. Ley. 2004. Lipopolysaccharide activation of the TPL-2/MEK/extracellular signal-regulated kinase mitogen-activated protein kinase cascade is regulated by IκB kinase-induced proteolysis of NF-κB1 p105. *Mol. Cell. Biol.* 24:9658–9667. http://dx.doi.org/10.1128/MCB.24.21.9658-9667.2004

Bulek, K., C. Liu, S. Swaidani, L. Wang, R.C. Page, M.F. Gulen, T. Herjan, A. Abbadi, W. Qian, D. Sun, et al. 2011. The inducible kinase IKKi is required for IL-17-dependent signaling associated with neutrophilia and pulmonary inflammation. *Nat. Immunol.* 12:844–852. http://dx.doi.org/10.1038/ni.2080

Chang, S.H., H. Park, and C. Dong. 2006. Act1 adaptor protein is an immediate and essential signaling component of interleukin-17 receptor. *J. Biol. Chem.* 281:35603–35607. http://dx.doi.org/10.1074/jbc.C600256200

Chang, M., W. Jin, and S.C. Sun. 2009. Peli1 facilitates TRIF-dependent Toll-like receptor signaling and proinflammatory cytokine production. *Nat. Immunol.* 10:1089–1095. http://dx.doi.org/10.1038/ni.1777

Compston, A., and A. Coles. 2008. Multiple sclerosis. *Lancet.* 372:1502–1517. http://dx.doi.org/10.1016/S0140-6736(08)61620-7

Dumitru, C.D., J.D. Ceci, C. Tsatsanis, D. Kontoyiannis, K. Stamatakis, J.H. Lin, C. Patriotis, N.A. Jenkins, N.G. Copeland, G. Kollias, and P.N. Tsichlis. 2000. TNF-α induction by LPS is regulated posttranscriptionally via a Tpl2/ERK-dependent pathway. *Cell.* 103:1071–1083. http://dx.doi.org/10.1016/S0092-8674(00)00210-5

Gaffen, S.L. 2009. Structure and signalling in the IL-17 receptor family. *Nat. Rev. Immunol.* 9:556–567. http://dx.doi.org/10.1038/nri2586

Gantke, T., S. Sriskantharajah, and S.C. Ley. 2011. Regulation and function of TPL-2, an IκB kinase-regulated MAP kinase kinase kinase. *Cell Res.* 21:131–145. http://dx.doi.org/10.1038/cr.2010.173

Garcia, A.D., N.B. Doan, T. Imura, T.G. Bush, and M.V. Sofroniew. 2004. GFAP-expressing progenitors are the principal source of constitutive neurogenesis in adult mouse forebrain. *Nat. Neurosci.* 7:1233–1241. http://dx.doi.org/10.1038/nn1340

Goverman, J. 2009. Autoimmune T cell responses in the central nervous system. *Nat. Rev. Immunol.* 9:393–407. http://dx.doi.org/10.1038/nri2550

Iwakura, Y., H. Ishigame, S. Saijo, and S. Nakae. 2011. Functional specialization of interleukin-17 family members. *Immunity.* 34:149–162. http://dx.doi.org/10.1016/j.immuni.2011.02.012

Jin, W., X.F. Zhou, J. Yu, X. Cheng, and S.C. Sun. 2009. Regulation of Th17 cell differentiation and EAE induction by MAP3K NIK. *Blood*. 113:6603–6610. http://dx.doi.org/10.1182/blood-2008-12-192914

Kang, Z., C.Z. Altuntas, M.F. Gulen, C. Liu, N. Giltiay, H. Qin, L. Liu, W. Qian, R.M. Ransohoff, C. Bergmann, et al. 2010. Astrocyte-restricted ablation of interleukin-17-induced Act1-mediated signaling ameliorates autoimmune encephalomyelitis. *Immunity*. 32:414–425. http://dx.doi.org/10.1016/j.immuni.2010.03.004

Liu, C., W. Qian, Y. Qian, N.V. Giltiay, Y. Lu, S. Swaidani, S. Misra, L. Deng, Z.J. Chen, and X. Li. 2009. Act1, a U-box E3 ubiquitin ligase for IL-17 signaling. *Sci. Signal*. 2:ra63. http://dx.doi.org/10.1126/scisignal.2000382

Matusevicius, D., P. Kivisäkk, B. He, N. Kostulas, V. Ozenci, S. Fredrikson, and H. Link. 1999. Interleukin-17 mRNA expression in blood and CSF mononuclear cells is augmented in multiple sclerosis. *Mult. Scler.* 5:101–104. http://dx.doi.org/10.1177/135245859900500206

Muls, N., K. Jnaoui, H.A. Dang, A. Wauters, J. Van Snick, C.J. Sindic, and V. van Pesch. 2012. Upregulation of IL-17, but not of IL-9, in circulating cells of CIS and relapsing MS patients. Impact of corticosteroid therapy on the cytokine network. *J. Neuroimmunol.* 243:73–80. http://dx.doi.org/10.1016/j.jneuroim.2011.12.010

Novatchkova, M., A. Leibbrandt, J. Werzowa, A. Neubüser, and F. Eisenhaber. 2003. The STIR-domain superfamily in signal transduction, development and immunity. *Trends Biochem. Sci.* 28:226–229. http://dx.doi.org/10.1016/S0968-0004(03)00067-7

Qian, Y., C. Liu, J. Hartupee, C.Z. Altuntas, M.F. Gulen, D. Jane-Wit, J. Xiao, Y. Lu, N. Giltiay, J. Liu, et al. 2007. The adaptor Act1 is required for interleukin 17-dependent signaling associated with autoimmune and inflammatory disease. *Nat. Immunol.* 8:247–256. http://dx.doi.org/10.1038/ni1439

Reiley, W.W., M. Zhang, W. Jin, M. Losiewicz, K.B. Donohue, C.C. Norbury, and S.C. Sun. 2006. Regulation of T cell development by the deubiquitinating enzyme CYLD. *Nat. Immunol.* 7:411–417. http://dx.doi.org/10.1038/ni1315

Roget, K., A. Ben-Addi, A. Mambole-Dema, T. Gantke, H.T. Yang, J. Janzen, N. Morrice, D. Abbott, and S.C. Ley. 2012. IκB kinase 2 regulates TPL-2 activation of extracellular signal-regulated kinases 1 and 2 by direct phosphorylation of TPL-2 serine 400. *Mol. Cell. Biol.* 32:4684–4690. http://dx.doi.org/10.1128/MCB.01065-12

Sato, S., H. Sanjo, K. Takeda, J. Ninomiya-Tsuji, M. Yamamoto, T. Kawai, K. Matsumoto, O. Takeuchi, and S. Akira. 2005. Essential function for the kinase TAK1 in innate and adaptive immune responses. *Nat. Immunol.* 6:1087–1095. http://dx.doi.org/10.1038/ni1255

Sawcer, S., G. Hellenthal, M. Pirinen, C.C. Spencer, N.A. Patsopoulos, L. Moutsianas, A. Dilthey, Z. Su, C. Freeman, S.E. Hunt, et al. Wellcome Trust Case Control Consortium 2. 2011. Genetic risk and a primary role for cell-mediated immune mechanisms in multiple sclerosis. *Nature*. 476:214–219. http://dx.doi.org/10.1038/nature10251

Schröfelbauer, B., S. Polley, M. Behar, G. Ghosh, and A. Hoffmann. 2012. NEMO ensures signaling specificity of the pleiotropic IKKβ by directing its kinase activity toward IκBα. *Mol. Cell.* 47:111–121.

Schwandner, R., K. Yamaguchi, and Z. Cao. 2000. Requirement of tumor necrosis factor receptor-associated factor (TRAF)6 in interleukin 17 signal transduction. *J. Exp. Med.* 191:1233–1240. http://dx.doi.org/10.1084/jem.191.7.1233

Serebrennikova, O.B., C. Tsatsanis, C. Mao, E. Gounaris, W. Ren, L.D. Siracusa, A.G. Eliopoulos, K. Khazaie, and P.N. Tsichlis. 2012. Tpl2 ablation promotes intestinal inflammation and tumorigenesis in Apcmin mice by inhibiting IL-10 secretion and regulatory T-cell generation. *Proc. Natl. Acad. Sci. USA*. 109:E1082–E1091. http://dx.doi.org/10.1073/pnas.1115098109

Shibuya, H., K. Yamaguchi, K. Shirakabe, A. Tonegawa, Y. Gotoh, N. Ueno, K. Irie, E. Nishida, and K. Matsumoto. 1996. TAB1: an activator of the TAK1 MAPKKK in TGF-β signal transduction. *Science*. 272:1179–1182. http://dx.doi.org/10.1126/science.272.5265.1179

Simmons, S.B., E.R. Pierson, S.Y. Lee, and J.M. Goverman. 2013. Modeling the heterogeneity of multiple sclerosis in animals. *Trends Immunol.* 34:410–422. http://dx.doi.org/10.1016/j.it.2013.04.006

Song, X., and Y. Qian. 2013. The activation and regulation of IL-17 receptor mediated signaling. *Cytokine*. 62:175–182. http://dx.doi.org/10.1016/j.cyto.2013.03.014

Spence, R.D., M.E. Hamby, E. Umeda, N. Itoh, S. Du, A.J. Wisdom, Y. Cao, G. Bondar, J. Lam, Y. Ao, et al. 2011. Neuroprotection mediated through estrogen receptor-α in astrocytes. *Proc. Natl. Acad. Sci. USA*. 108:8867–8872. http://dx.doi.org/10.1073/pnas.1103833108

Sugimoto, K., M. Ohata, J. Miyoshi, H. Ishizaki, N. Tsuboi, A. Masuda, Y. Yoshikai, M. Takamoto, K. Sugane, S. Matsuo, et al. 2004. A serine/threonine kinase, Cot/Tpl2, modulates bacterial DNA-induced IL-12 production and Th cell differentiation. *J. Clin. Invest.* 114:857–866. http://dx.doi.org/10.1172/JCI20014

Sun, D., M. Novotny, K. Bulek, C. Liu, X. Li, and T. Hamilton. 2011. Treatment with IL-17 prolongs the half-life of chemokine CXCL1 mRNA via the adaptor TRAF5 and the splicing-regulatory factor SF2 (ASF). *Nat. Immunol.* 12:853–860. http://dx.doi.org/10.1038/ni.2081

Vougioukalaki, M., D.C. Kanellis, K. Gkouskou, and A.G. Eliopoulos. 2011. Tpl2 kinase signal transduction in inflammation and cancer. *Cancer Lett.* 304:80–89. http://dx.doi.org/10.1016/j.canlet.2011.02.004

Waterfield, M.R., M. Zhang, L.P. Norman, and S.C. Sun. 2003. NF-κB1/p105 regulates lipopolysaccharide-stimulated MAP kinase signaling by governing the stability and function of the Tpl2 kinase. *Mol. Cell.* 11:685–694. http://dx.doi.org/10.1016/S1097-2765(03)00070-4

Waterfield, M., W. Jin, W. Reiley, M.Y. Zhang, and S.-C. Sun. 2004. IκB kinase is an essential component of the Tpl2 signaling pathway. *Mol. Cell. Biol.* 24:6040–6048. http://dx.doi.org/10.1128/MCB.24.13.6040-6048.2004

Watford, W.T., B.D. Hissong, L.R. Durant, H. Yamane, L.M. Muul, Y. Kanno, C.M. Tato, H.L. Ramos, A.E. Berger, L. Mielke, et al. 2008. Tpl2 kinase regulates T cell interferon-gamma production and host resistance to *Toxoplasma gondii*. *J. Exp. Med.* 205:2803–2812. http://dx.doi.org/10.1084/jem.20081461

Xiao, Y., J. Jin, M. Chang, J.H. Chang, H. Hu, X. Zhou, G.C. Brittain, C. Stansberg, O. Torkildsen, X. Wang, et al. 2013. Peli1 promotes microglia-mediated CNS inflammation by regulating Traf3 degradation. *Nat. Med.* 19:595–602. http://dx.doi.org/10.1038/nm.3111

Zepp, J., L. Wu, and X. Li. 2011. IL-17 receptor signaling and T helper 17-mediated autoimmune demyelinating disease. *Trends Immunol.* 32:232–239. http://dx.doi.org/10.1016/j.it.2011.02.007

Zhu, S., W. Pan, X. Song, Y. Liu, X. Shao, Y. Tang, D. Liang, D. He, H. Wang, W. Liu, et al. 2012. The microRNA miR-23b suppresses IL-17-associated autoimmune inflammation by targeting TAB2, TAB3 and IKK-α. *Nat. Med.* 18:1077–1086. http://dx.doi.org/10.1038/nm.2815